Received: 18 May 2023 | Revised: 3 July 2023 | Accepted: 16 July 2023

DOI: 10.1002/ajh.27044

RESEARCH ARTICLE

Sequencing-based analysis of clonal evolution of 25 mantle cell lymphoma patients at diagnosis and after failure of standard immunochemotherapy

J. Karolová[1,2] | D. Kazantsev[1] | M. Svatoň[3] | L. Tušková[1] | K. Forsterová[2] | D. Maláriková[1,2] | K. Benešová[2] | T. Heizer[1] | A. Dolníková[1] | M. Klánová[1,2] | L. Winkovska[3] | K. Svobodová[4] | J. Hojný[5] | E. Krkavcová[5] | E. Froňková[3] | Z. Zemanová[4] | M. Trněný[2] | P. Klener[1,2]

[1]Institute of Pathological Physiology, First Faculty of Medicine, Charles University, Prague, Czech Republic

[2]First Department of Medicine – Hematology, University General Hospital Prague and First Faculty of Medicine, Charles University, Prague, Czech Republic

[3]CLIP – Childhood Leukaemia Investigation Prague, Department of Pediatric Haematology and Oncology, Second Faculty of Medicine, Charles University and University Hospital Motol, Prague, Czech Republic

[4]Center for Oncocytogenetics, Institute of Medical Biochemistry and Laboratory Diagnostics, Charles University and General University Hospital, Prague, Czech Republic

[5]Institute of Pathology, First Faculty of Medicine, Charles University and General University Hospital, Prague, Czech Republic

Correspondence
P. Klener, Institute of Pathological Physiology, First Faculty of Medicine, Charles University, U Nemocnice 5, Prague 2, 12853, Czech Republic.
Email: pavel.klener2@lf1.cuni.cz; pavel.klener2@vfn.cz

Funding information
Cooperatio Program, Research Area "Hematooncology" and Charles University Graduate Students Research Program (Acronym SVV), Grant/Award Number: 260634/2023; Czech Health Research Council, Grant/Award Number: AZV NU21-03-00386; Czech Republic, Grant/Award Number: GA23-05377S; Ministry of Health, Czech Republic, Grant/Award Number: MH CZ-DRO-VFN64165; European Union – Next Generation EU, Grant/Award Number: LX22NPO5102

Abstract

Our knowledge of genetic aberrations, that is, variants and copy number variations (CNVs), associated with mantle cell lymphoma (MCL) relapse remains limited. A cohort of 25 patients with MCL at diagnosis and the first relapse after the failure of standard immunochemotherapy was analyzed using whole-exome sequencing. The most frequent variants at diagnosis and at relapse comprised six genes: *TP53*, *ATM*, *KMT2D*, *CCND1*, *SP140*, and *LRP1B*. The most frequent CNVs at diagnosis and at relapse included *TP53* and *CDKN2A/B* deletions, and *PIK3CA* amplifications. The mean count of mutations per patient significantly increased at relapse ($n = 34$) compared to diagnosis ($n = 27$). The most frequent newly detected variants at relapse, *LRP1B* gene mutations, correlated with a higher mutational burden. Variant allele frequencies of *TP53* variants increased from 0.35 to 0.76 at relapse. The frequency and length of predicted CNVs significantly increased at relapse with *CDKN2A/B* deletions being the most frequent. Our data suggest, that the resistant MCL clones detected at relapse were already present at diagnosis and were selected by therapy. We observed enrichment of genetic aberrations of DNA damage response pathway (*TP53* and *CDKN2A/B*), and a significant increase in MCL heterogeneity. We identified *LRP1B* inactivation as a new potential driver of MCL relapse.

1 | INTRODUCTION

Mantle cell lymphoma (MCL) is a heterogeneous disease characterized by a chronically relapsing clinical course.[1,2] Despite the implementation of several innovative drugs and adoptive immunotherapy with genetically modified autologous T-lymphocytes into clinical practice, the standard front-line therapy for patients with newly diagnosed MCL is still based on immunochemotherapy with or without high-dose therapy, and autologous stem cell transplantation.[3] In the last decade, whole exome sequencing (WES) of large unbiased cohorts of newly diagnosed MCL patients enabled not only the identification of driver genetic lesions (variants, copy number variants) but also genetic profiles associated with clinical outcome.[4–15] In contrast, our knowledge on the clonal evolution of MCL after the failure of standard immunochemotherapy remains limited.[7,16]

In this study, we used WES to study mutational profiles of 25 patients with MCL, who experienced relapse or progression after standard front-line immunochemotherapy.

2 | METHODS

2.1 | Patients and samples

Lymphoma samples were collected from 25 patients with newly diagnosed MCL (75% male) following patients' informed consent and according to the declaration of Helsinki. Tumor tissue samples were collected at the time of lymphoma diagnosis, and at the time of disease relapse. Non-tumorous (germline) samples collected using buccal smears or trephine biopsies without tumorous infiltration were obtained from all patients to filter out gene polymorphisms. Only tumor tissue samples with tumorous infiltration ≥30% according to flow cytometry were included in the analysis. The study was approved by the Ethics Committee of the General University Hospital at Prague under No. 60/20.

2.2 | Next-generation exome sequencing and copy number variant analysis

Genomic DNA was extracted using DNeasy Blood & Tissue Kit (Qiagen, Germany) according to the manufacturer's protocol. Samples were sequenced on the NextSeq 500 instrument (Illumina, San Diego, CA) according to the manufacturer's protocols with sequencing libraries prepared using SureSelectXT Human All Exon V6 + UTR kit (Agilent Technologies, Santa Clara, CA). The resulting reads were then aligned against the human reference genome (build GRCh37). All alignments were performed by BWA.[17] Mean coverage per sample was 66 reads. Genomic variants were called with samtools and VarScan 2.[18,19] Variant annotation was performed using SnpEff.[20] Only nonsynonymous variants in the gene coding regions with coverage of at least 10 reads with mapping quality and base quality scores higher than 20 in related samples from each patient were compared together based on their frequency. Variants present in the patient's germline DNA at a frequency higher than 0.05 were excluded from analysis in all cases. We compared variants with an allele frequency ≥0.1 in at least one of the compared samples that were present in at least three reads in both, diagnostic and relapsed sample. Both the filtering of variants and plotting of counts and frequencies of variants was done in RStudio. The variants were manually reviewed in Integrative Genomics Viewer to exclude sequencing artifacts or variants present but not called in the germline sample.[21,22] "Oncoprint" function from the ComplexHeatmap R package was used to visualize detected variants.[23] Resulting plots show variants present in at least two patients. Mutations of *TP53* were plotted on a lollipop plot using the maftools package.[24] A complete list of variants filtered out are available at the Table S1.

Copy number variants (CNVs) were predicted using CNVkit and a pooled reference from normal control samples.[25,26] Genomic segments were identified as amplifications or deletions based on their allelic copy numbers. We used the "weight" value from the CNVkit output as a metric that combines both segment length and sequencing coverage. The "Genomic Identification of Significant Targets in Cancer" (GISTIC[27]) was used for assigning the statistical significance to the amplified and deleted segments identified by CNVkit. The broad GISTIC algorithm was used to find significantly altered copy numbers on the levels of chromosome arm regions and of individual genes. To generate color-coded heatmaps, these genes were filtered out using a CNV gene list of 22 genes (Table S1).[4–7,9,11,13–16,28–32] An overview of data processing pipelines is shown in Figure S1.

Note: One of the 25 patients (P25) analyzed in the study was sequenced by Atlas Biolabs (Berlin, DE) with libraries prepared using Nimblegen SeqCap ERZ Human Exome Library v 2.0 (Roche Nimblegen, Madison, WI) on the HiSeq 2000 (Illumina, San Diego, CA) instrument. Data for the CNV analysis from this patient were not available at the time of the analysis. Therefore, the CNV analysis was performed on 24 out of 25 patients.

2.3 | Targeted next-generation sequencing

For details, see Supplementary Materials—Methods.

2.4 | TaqMan copy number assay

TaqMan Copy Number Reference Assay RNase P (ThermoFisher scientific) was performed according to the manufacturer's instructions. Following probes were used: PIK3CA Hs02661768_cn, and CDKN2A Hs01354804_cn.

Briefly, DNA was diluted to the concentration of 5 ng/μL in nuclease-free water and stored at −20°C. The reporter dye of the Copy Number Assay primers was FAM w/o quencher, and the reporter dye of the Copy Number Reference Assay was VIC with TAMRA probe quencher. The assay was completed by a QuantStudio 7 Pro PCR analyzer (ThermoFisher Scientific) and had 40 cycles with the denaturing steps at 95°C for 15′ and the annealing steps at 60°C for 60′.

Signal from the samples was thresholded to the signal of RNAse P and cycle threshold difference (dCT) was calculated as $(CT_{sample} - CT_{control})$. Allele copy number was then calculated as 2×2^{-dCT}.

2.5 | Fluorescence in situ hybridization

As a part of standard baseline diagnostic procedures, interphase fluorescence in situ hybridization (FISH) detecting 9p and 17p deletions were implemented in patients at diagnosis using the Vysis LSI CDKN2A/CEP 9 FISH Probe Kit (Abbott Molecular, Des Plaines, IL, USA) and XL ATM/TP53 Deletion Probe (MetaSystems, Altlussheim, Germany) according to the manufacturer's protocols. At least 200 interphase nuclei were analyzed per probe by two independent observers. The cut-off level for positive values were determined on samples obtained from 10 cytogenetically normal persons and were found to be 5% (mean ± 3SD) for losses (deletions, monosomies).

2.6 | Statistical analyses

Statistical analysis was carried out with GraphPad version 5 (GraphPad Prism version 5.00 for Windows, GraphPad Software, La Jolla, CA, USA, www.graphpad.com) and with R version 4.2.1 and RStudio 2022.07.1 (R Core Team [2021]. R: A language and environment for statistical computing. R Foundation for Statistical Computing, Vienna, Austria, https://www.R-project.org/).

Means of counts of shared, N/D and N/U mutations were compared using non-paired Student's *t*-test with *p* values adjusted using the Holm method. The same test was used to compare means of CNV weights for amplifications and deletions at relapse versus at diagnosis. Means of counts of SNVs at diagnosis and at relapse were compared using paired Student's *t*-test. Means of counts of SNVs at relapse in patients with and without LRP1B mutation were compared using unpaired Student's *t*-test.

Event-free survival (EFS) and overall survival (OS) were estimated with Kaplan–Meier statistics. EFS was defined as the time between the date of treatment start to the date of lymphoma relapse, progression, or death due to any cause or start of new anti-lymphoma treatment. If a patient has not progressed or died or started a new anti-lymphoma treatment at the analysis cut-off date, EFS was censored on the date of last contact. OS was defined as the time between the date of treatment start to the date of death due to any cause. If a patient has not died at the analysis cut-off date, OS was censored on the date of last contact.

3 | RESULTS

3.1 | Baseline characteristics and clinical outcome of MCL patients

Baseline characteristics of the analyzed patients are displayed in Table 1. Briefly, 75% of patients were men (median = 68 years, range 47–81 years), 84% had high-risk disease according to MIPI, 59% had adverse morphology (pleomorphic or blastoid), and 56% high proliferation index by Ki-67 (≥30%). Fifty-six percent of patients were treated with R-CHOP-like regimens, and 44% received intensified treatments (for details, see Table 1).[33,34] The best response to front-line therapy is shown in Table 1. Briefly, response assessed by CT or PET-CT (i.e., complete, or partial remission = CR or PR) was observed in 23 out of 25 patients, stable disease (SD) was observed in two patients. The median EFS and OS for the whole cohort were 10 months (1.3–90.6 months) and 29 months (9.5–109.5 months), respectively.

3.2 | Genetic alterations identified by WES

A rigorous filtration process of the dataset revealed 922 non-synonymous variants (referred to as "variants"), 90% of which were single-nucleotide variants (SNVs), the rest was represented by small indels. Overall, 616 variants were detected both at the diagnostic (DG) and relapsed samples (REL) (i.e., shared variants). In addition, 236 and 70 variants were newly detected (N/D), and newly undetected (N/U), respectively, at relapse compared to diagnosis. There were 24.6 ± 1.7 (mean ± SEM) shared variants per patient between the diagnostic and relapsed sample. There were 9.8 ± 1.9 newly detected variants at relapse (N/D) and only 3.5 ± 0.8 newly undetected variants at relapse (N/U), which is significantly lower ($p < .0001$; Figure S2A). Consequently, the total mean count of variants per patient was significantly higher at relapse (34.1 ± 2.9) compared to diagnosis (27.4 ± 1.8, $p < .001$) (Figure S2B). Detailed overview of counts of shared, N/D and N/U variants for each patient is shown in a stacked bar plot at Figure S3A.

The mutational pattern between the diagnostic and relapsed samples remained similar and comprised predominantly missense variants (82.7% at diagnosis and 83.1% at relapse), stop-gained variants (7.1% at diagnosis and 7.0% at relapse), and frameshift variants (6.9% at diagnosis and 6.6% at relapse). The most frequent substitutions at both diagnostic and relapsed samples were transitions (Figure S2C,D). Prediction of variant's impact by SnpEff toolbox revealed 97 high-impact mutations (i.e., frameshift and stop-gained variants) at diagnosis and 117 at relapse, respectively (20.6% increase at relapse). Most of the variants were predicted to have moderate impact (i.e., missense variants, inframe deletions), namely 583 at diagnosis, and 727 at relapse (24.7% increase at relapse; Figure S2E).

3.3 | Mutational profile of MCL patients at diagnosis

The most frequently mutated gene at diagnosis was the tumor suppressor *TP53* (mutated in 12 out of 25 patients, 48%), followed by *ATM* (8 patients, 32%), *KMT2D* (7 patients, 28%), *CCND1* and *SP140* (each in 5 patients, 20%), and *LRP1B* (4 patients, 16%) genes. Six genes were found mutated in 3 out of 25 patients (12%): *NFKBIE*, *ARFGEF3*, *NOTCH1*, *TRAF2*, *CASP5*, and *SMARCA4* (Figure 1A). Additional 36 genes were mutated in ≥2 out of 25 patients (Figure S4). The majority of *TP53* variants were localized in the p53 DNA binding domain (9/12, 75%), two in the p53 tetramerization motif (2/12, 17%) and one in the untranslated region (Figure 2D). Of note, mutations of

TABLE 1 Characteristics of patients at diagnosis.

Code	Age	Sex	MIPI	Morphology	Ki-67 (%)	Therapy	ASCT	Best response to front-line Tx	EFS (months)	OS (months)	Death
P01	74	M	6.4	Pleomorphic	80	1A	0	PR	5	11	Y
P02	66	M	6.9	N/A	N/A	2A	1	CR	50	82	N
P03	60	M	5.7	Blastoid	60	2A	1	CR	10	15	Y
P04	47	F	7.3	Classic	90	2A	1	CR	7	10	Y
P05	79	F	7.0	Blastoid	75	1A	0	SD	1	26	Y
P06	79	M	6.8	N/A	<5	1A	0	CR	35	37	Y
P07	74	M	6.1	N/A	N/A	1A	0	CR	10	29	Y
P08	48	M	5.4	Classic	10–20	2A	1	CR	91	104	N
P09	78	F	6.6	Classic	25	1A	0	CR	16	33	Y
P10	73	F	6.9	N/A	15	1A	0	CR	66	102	N
P11	68	M	6.8	N/A	7.5	1A	0	PR	15	29	Y
P12	74	M	7.9	Blastoid	75	1A	0	CR	12	12	Y
P13	69	M	7.0	Blastoid	80	1A	1	PR	7	10	Y
P14	67	M	6.3	Blastoid	85	2B	1	PR	8	17	Y
P15	62	M	7.0	Classic	25	1A	0	PR	6	70	Y
P16	68	M	8.0	Pleomorphic	90	1B	0	PR	4	31	Y
P17	69	F	6.4	Pleomorphic	60	3	0	PR	3	10	Y
P18	63	M	7.0	Blastoid	100	2A	0	CR	4	10	Y
P19	65	M	6.2	Pleomorphic	40	2A	0	CR	53	110	N
P20	76	M	7.3	N/A	100	1A	0	CR	10	12	Y
P21	81	M	7.5	Classic	5	1A	0	SD	1	33	Y
P22	68	M	5.9	N/A	5	1A	0	CR	25	42	Y
P23	66	M	7.1	Classic	70	2A	1	PR	9	11	Y
P24	70	M	6.4	N/A	40	1A	0	CR	30	104	N
P25	55	M	5.5	Classic	5	2A	1	PR	10	20	Y

Note: Therapy: 1A = Czech lymphoma study group (CLSG)-MCL1 observational protocol,[62] that is, alternation of R(ituximab)-CHOP (cyclophosphamide, doxorubicin, vincristine, and prednisone), and R-high-dose cytarabine (HDAC, 2 g/m^2, 2 doses every 24 h), 3 + 3 cycles, and rituximab maintenance (RM); 1B = modification of CLSG-MCL1 protocol, that is, alternation of R-CHOP and R-DHAOx-senior (dexamethasone, HDAC, reduced oxaliplatin), 3 + 3 cycles, and RM; 2A = Nordic protocol,[34] that is, alternation of R-Maxi-CHOP, and R-HDAC (2–3 g/m^2, 4 doses every 12 h), 3 + 3 cycles, autologous stem cell transplant (ASCT), and RM; 2B = modified Nordic protocol, that is, alternation of R-Maxi-CHOP, and R-DHAOx, 3 + 3 cycles, and RM; 3 = R-COP.

Abbreviations: 0, no; 1, yes; ASCT, autologous stem cell transplantation; CR, complete remission; EFS, event-free survival; F, female; HD, high dose; M, male; N, no; N/A, not analyzed; OS, overall survival; P, patient; PR, partial remission; SD, stable disease; Tx, therapy; Y, yes.

TP53 retained a trend of unfavorable prognostic significance even in this preselected cohort of relapsed MCL patients (Figure S5, part 5A).

3.4 | Predicted CNV profile of MCL patients at diagnosis

Significant arm-level CNVs at diagnosis (i.e., frequency score > 0.15, *q* value < 0.01) included deletions located on chromosomal arms 9p, 9q, 13q, and 17p, and an amplification on 3q (Figure 2A). On the gene-level, 20/22 genes from the CNV gene list were altered in ≥2 patients at diagnosis (Figure 1B). The most common was the deletion of one of the regulators of PI3K-AKT pathway guanine nucleotide binding protein alpha 14 (*GNA14*, see also Figure S6), predicted in 12 out of 24 patients (50%), followed by deletions of *TP53*, *ANXA1*, *ALDH1A1*, *MIR15A*, and *MIR16.1* in 11 patients (46%). Combining these data with the mutational profile, *TP53* inactivation at diagnosis was found in 16 out of 25 patients (64%). Seven patients (29%) had both the mutation and deletion of *TP53*. *CDKN2A*, *RB1*, *NOTCH1*, *RHOBTB2*, *SORBS3*, and *TNFRSF10B* genes were each deleted in 10 patients at diagnosis (42%). Sixteen genes from the CNV gene list were deleted in more than six patients at diagnosis. The most frequently observed amplifications included copy number gains of *PIK3CA* and *SOX2* (46%) followed by *MYC* (9 patients, 37.5%), and *BCL2* (5 patients, 20%) (Figure 1B).

The WES-based CNV predictions for *TP53* and *CDKN2A* were independently evaluated by FISH implemented as a part of standard baseline diagnostic procedures in 24 out of 25 patients. In the majority of cases (91%), FISH confirmed the WES-based CNV predictions of *CDKN2A* and *TP53* deletions (Figure S7).

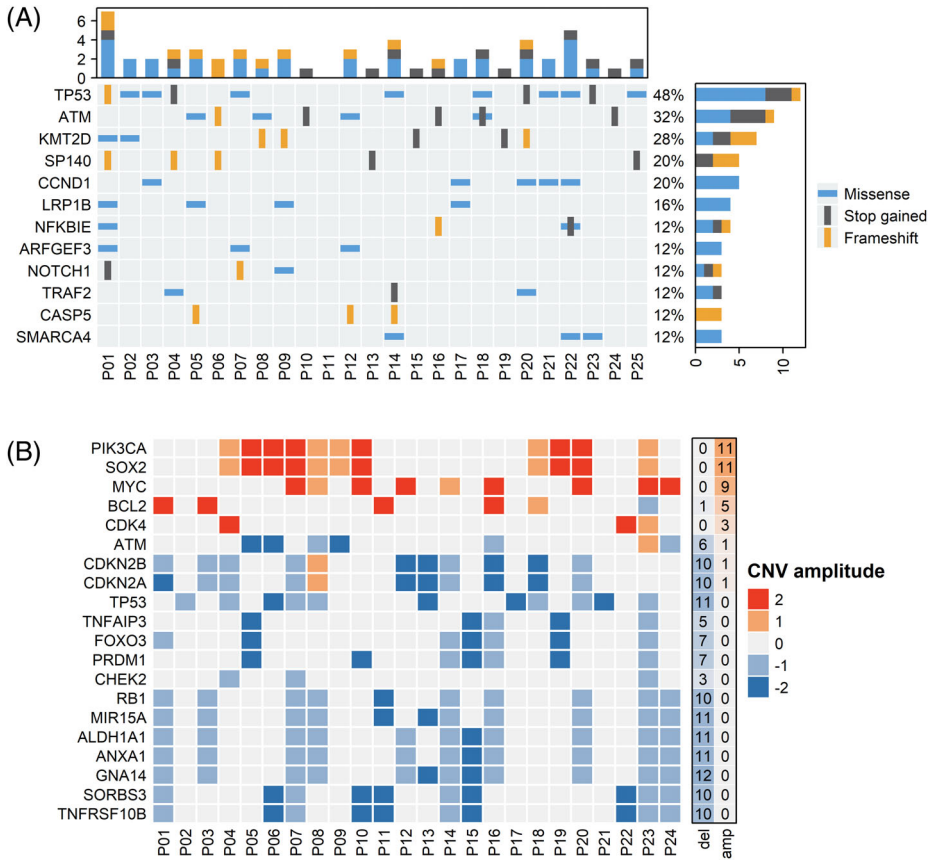

FIGURE 1 Mutational profile and copy number variation (CNV) profile of mantle cell lymphoma patients at diagnosis: (A) Oncoprint of detected variants at diagnosis present at ≥3 patients. Upper bar plot showing number and type of variants per patient. Right-sided bar plot showing percentage and type of a variant per specified gene. (B) Heatmap showing copy number (CN) variation on a level of individual genes. Genes were filtered against our pre-compiled CNV gene list. CN values were thresholded using GISTIC and are expressed as amplitudes of divergence from control. Sum of cases of CNVs for a given gene is plotted on the right side of the heatmap. P, patient. [Color figure can be viewed at wileyonlinelibrary.com]

3.5 | Mutational profile of MCL patients at relapse

The majority of variants detected at diagnosis were also detected at lymphoma relapse. The most prevalent mutation detected at lymphoma relapse remained a mutation of *TP53* detected in 48% of patients. The other most prevalent variants at relapse comprised mutations of *ATM*, *KMT2D*, and *LRP1B* (Figure 3A). Even though no new mutations of *TP53* were detected at relapse, the median variant allele frequency (VAF) of *TP53* mutations significantly increased at relapse (0.76) compared to diagnosis (0.35) (Figure 2C).

Several variants were newly detected at lymphoma relapse and were not detected at diagnosis. The most frequent newly detected variant at relapse was a mutation of *LRP1B* gene (three new variants in two new patients). In total, 6 out of 25 patients (24%) harbored a mutation of *LRP1B* at relapse (one patient had two variants of *LRP1B* gene; Figure 3A). As previously shown for other malignancies, mutations of *LRP1B* at relapse significantly correlated with higher total mutation burden in MCL and at diagnosis had a trend toward shorted OS (Figure S5, part 5B and Figure S8). Other newly detected variants comprised mutations of *KMT2D*, *HOXD9*, *CDC27*, *RYR2*, and *FLNA* genes (each newly mutated in two patients) (Figure S3B). Complete mutational profile of variants found at relapse in at least two patients is shown in Figure S9. Of note, from the list of significantly mutated genes at diagnosis (i.e., genes mutated in ≥2 patients), five genes were newly mutated in one additional patient at relapse including *ATM*, *CASP5*, *ETNK1*, *LRRIQ1*, and *NOTCH2*.

3.6 | Predicted CNV profile of MCL patients at relapse

Compared to diagnosis, arm-level events consisted of one newly amplified chromosome arm (7p) and three newly deleted chromosome arms (6q, 8p, and 21p). All chromosomal arms significantly altered at diagnosis ($q < 0.01$) were significantly altered at relapse (Figure 2A).

The majority of CNV changes detected at diagnosis were also observed at relapse. However, deletions and amplifications detected at relapse were more frequent, and were larger in scale (i.e., had bigger weight, $p < 0.05$; Figure 2B). The most prevalent alterations at lymphoma relapse were deletions of *CDKN2A* and *CDKN2B* genes, newly predicted in 8 patients (in total 18 out of 24 analyzed patients at relapse, 75%; Figure 3B). In univariate analysis, the predicted *CDKN2A* deletions (at diagnosis) correlated with significantly shorted OS even within our selected cohort of relapsed MCL patients (Figure S5, part 5C). Deletions of *TP53* were newly detected in four patients, and not detected in one (in total 14 out of 24 patients at relapse, 58%). The total number of patients with *TP53* gene inactivation (i.e., a mutation and/or deletion) at relapse was 19 (76%). Of these, seven patients had both a mutation and a deletion (P02, P04, P07, P18, P20, P21, and P22), five patients had isolated mutation (P01, P03, P14, P23, and P25) and seven patients had isolated deletion of *TP53* (P06, P08, P10, P12, P13, P17, P19). *ATM* deletions were newly predicted in three patients (in total 9 out of 24 patients, 37.5%)—seven patients had both a mutation and a deletion of *ATM*

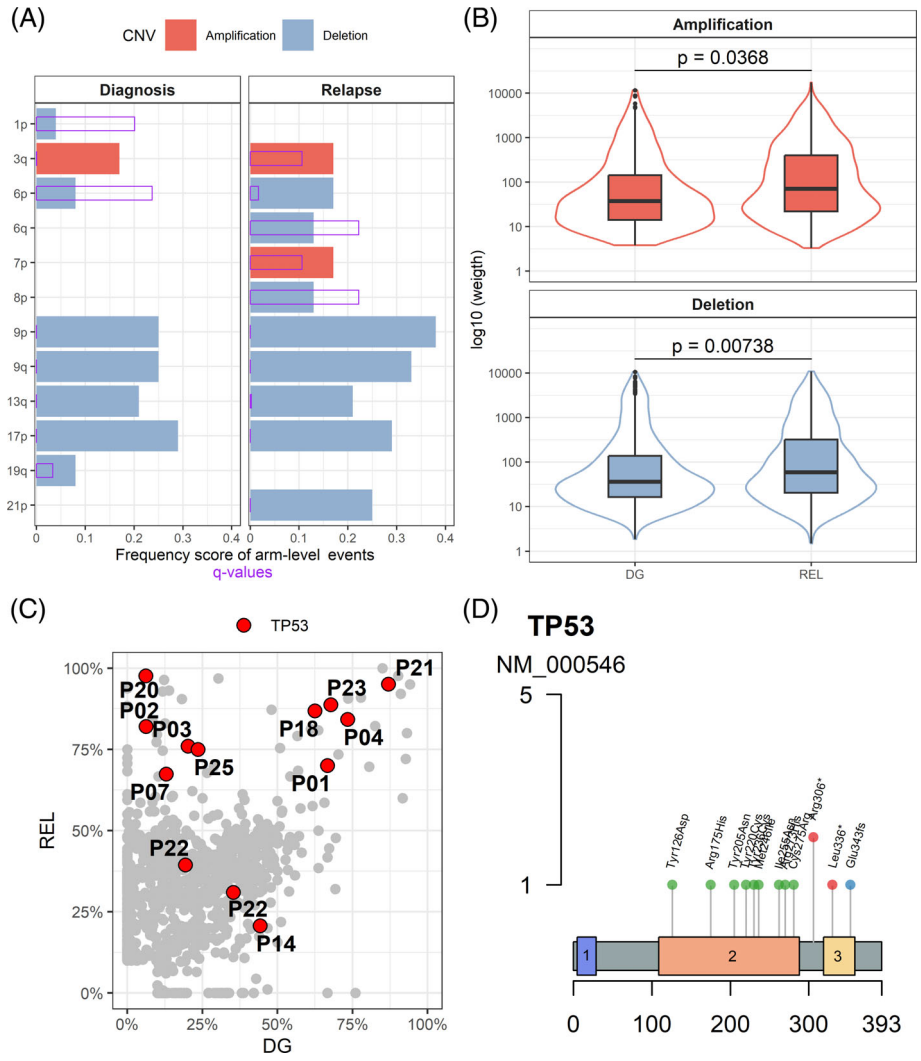

FIGURE 2 CNV profile and evolution at relapse compared to diagnosis, *TP53* mutations—development of variant allele frequency from diagnosis to relapse and localization of *TP53* mutations. (A) Comparison of chromosome arm-level CNVs at diagnosis and relapse, *q* values ≤0.25 are statistically significant (i.e., false positive ratio). (B) Comparison of CNV weight of the amplified and deleted regions between diagnostic and relapsed samples with calculated *p*-value (unpaired *t*-test). (C) Variant allele frequency (VAF) of TP53 (red) with all the shared, newly detected, and newly undetected variants (light gray) between diagnostic and corresponding relapsed sample in all patients. (D) Structural localization of TP53 mutations detected by whole exome sequencing. 1 = Purple box = *P53*—transactivation motif, 2 = Orange box = *P53*—DNA binding domain, 3 = Yellow box = *P53*—tetramerisation motif. CNV, copy number variation; DG, diagnosis; P, patient; REL, relapse. [Color figure can be viewed at wileyonlinelibrary.com]

(P05, P06, P08, P10, P12, P16, P24), two patients had isolated mutation of *ATM* (P17, P20) and three patients had isolated deletion of *ATM* (P01, P09, P17). Of note, *ATM* mutations and/or deletions at diagnosis did not show an impact on OS. On the contrary, there was a trend to a better OS (Figure S5, part 5D). The most frequent gains among the genes from the CNV gene list at relapse included *PIK3CA* (12 out of 24 patients, 50%), *SOX2* (11 out of 24 patients, 46%), *MYC* (9 out of 24 patients, 37.5%), and *BCL2* (7 out of 24 patients, 29%).

The predicted *CDKN2A* deletions, and *PIK3CA* gains at relapse were independently evaluated in patients with available DNA samples (i.e., 12 and 14 out of 25, respectively) by specific TaqMan DNA copy number assays (Figure S10). WES-based CNV predictions of the *CDKN2A* and *PIK3CA* alterations were confirmed by TaqMan DNA copy number assay in 86% and 88% of cases, respectively.

4 | DISCUSSION

In this study, we analyzed mutational profiles of 25 MCL patients at diagnosis and after failure of front-line immunochemotherapy using WES. To the best of our knowledge, the analyzed cohort represents one of the largest sequential analyses of MCL to date.[5] Importantly, the analyzed cohort did not represent a random selection of newly diagnosed MCL, but comprised only patients, who experienced lymphoma relapse. Therefore, overrepresentation of adverse prognostic factors at lymphoma diagnosis, including high numbers of cases with advanced MIPI, aggressive morphology (pleomorphic or blastoid), high proliferation rate by Ki-67, and high mutation rate of *TP53* were observed. Consequently, the median EFS and OS of the whole cohort were 10, and 29 months, respectively.

The most frequently mutated gene at diagnosis was the tumor suppressor *TP53* altered in 48% of patients. Of note, the presence of *TP53* mutation at diagnosis was associated with a trend of shorted OS, although it did not reach statistical significance in our cohort of 25 patients.

The most significant arm-level CNVs comprised among others del(9p), del(13q), and del(17p) encompassing known tumor suppressor genes *CDKN2A/B*, *RB1*, and *TP53*. Genetic profile of the analyzed MCL patients at diagnosis thus resembled a recently described prognostically unfavorable C4 cluster with a combination of del(17p)/*TP53* mutations, del(13q), and del(9p), with a hyperproliferative signature and 5-year OS of 14.2%.[16]

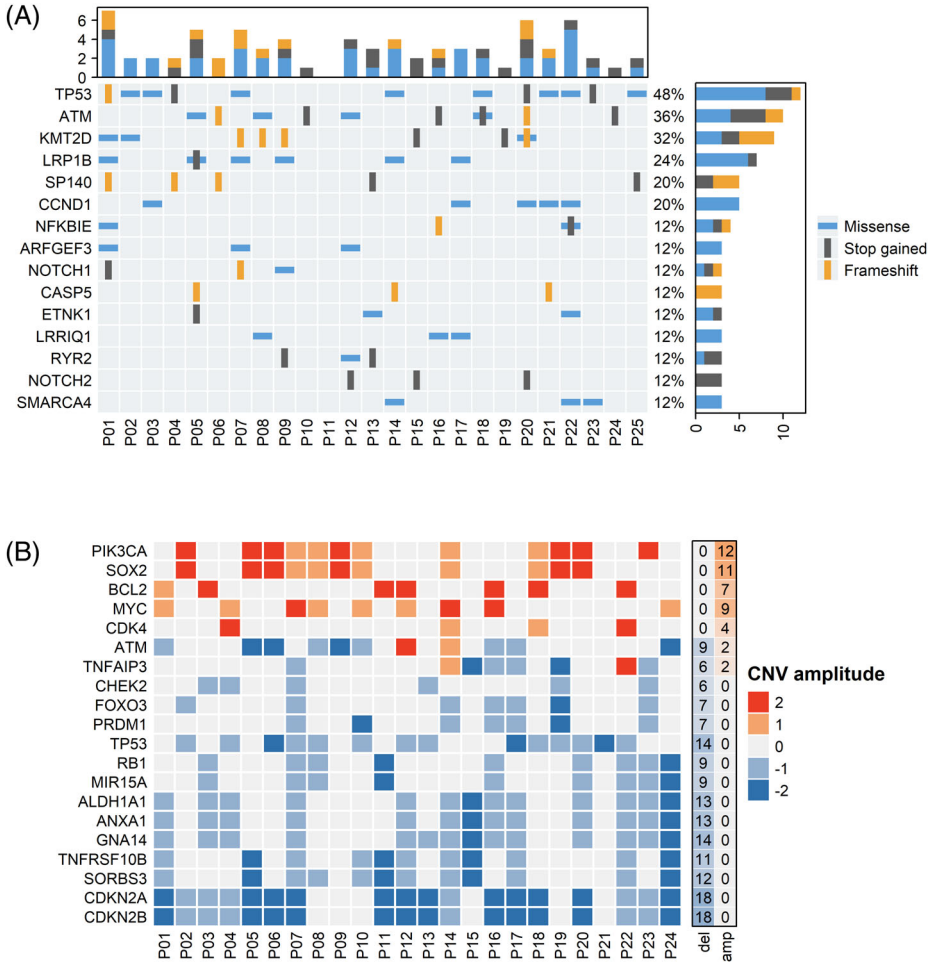

FIGURE 3 Mutational profile and copy number variations (CNV) profile of mantle cell lymphoma patients at relapse: (A) Oncoprint of detected variants at relapse present at ≥3 patients. Upper bar plot showing number and type of variants per patient. Right-sided bar plot showing percentage and type of a variant per specified gene. (B) Filtered CNVs at the time of the relapse. Genes were filtered against our pre-compiled CNV gene list. CN values were thresholded using GISTIC and are expressed as amplitudes of divergence from control. Sum of cases of CNVs for a given gene is plotted on the right side of the heatmap. [Color figure can be viewed at wileyonlinelibrary.com]

Compared to so far published results obtained from various unselected cohorts of newly diagnosed MCL patients, our WES data were markedly enriched in prognostically adverse variants already at diagnosis.[4,5,7,16,28–31,35–37] Besides the observed high numbers of cases with mutated *TP53*, mutations of *KMT2D* were found in 28% of patients, mutations of *SP140* in 20% patients, mutations of *NOTCH1* or *NOTCH2* in 24% patients, and predicted deletions of *CDKN2A/B* in 40% patients (Table S2).[4,5,7,10,16,28] The data suggest that the observed high prevalence of the established adverse aberrations already at diagnosis facilitate selection of therapy resistant MCL clones (with subsequent clinical relapse), which at least partially explains the relative scarcity of de novo detected mutations at lymphoma relapse.

Of note, with a single exception, mutations of *TP53* and *ATM* were mutually exclusive suggesting different biological subgroups of MCL patients. Indeed, while mutations of *TP53* correlated with a trend to significantly shorted OS, mutations of *ATM* had a trend toward better OS (though not statistically significant).[4,38–40] While mutations of prognostically adverse genes (i.e., *TP53*, *KMT2D*, *SP140*, or *NOTCH1/2*) were without exception enriched in our cohort compared to unselected cohorts of newly diagnosed MCL, mutations of *ATM* were underrepresented in our analysis (32%) compared to the so far published data (34%–44%; Table S2).

From a broad perspective, the vast majority of variants and CNVs detected at diagnosis were also detected at relapse. In addition, MCL cells at relapse harbored several newly detected variants, and more and larger CNVs, which demonstrates a striking increase in genetic heterogeneity of the chemotherapy-resistant lymphoma populations. There are two potential mechanisms by which the analyzed MCL populations at relapse might gain higher genetic heterogeneity compared to the diagnostic samples (i.e., more variants, and larger and more CNVs). Either the chemotherapy selected MCL (sub)clones with frequent *TP53* and *CDKN2A/B* inactivation are more genetically heterogeneous already at the time of therapy, or they become more genetically heterogeneous at the time of lymphoma relapse because they are more prone to acquisition of additional genetic mutations and CNVs due to inactivation of DNA damage response pathways. This question can be answered only by single-cell OMICs approaches.

The most frequent genetic aberrations detected at lymphoma relapse comprised mutations and deletions of *TP53* (76% of cases), and deletions of *CDKN2A/B* (75% of cases). Except for two patients (P9 and P15), all the analyzed patients at relapse had either aberration of *TP53* or deletion of *CDKN2A/B*. Of note, both patients, P9 and P15, harbored a concurrent mutation of *KMT2D*, and either *NOTCH1* or *NOTCH2*, that is, two other well-established driver genes in MCL.[7,10,12,41]

Despite that no new mutations of *TP53* were detected at relapse, median VAF of *TP53* mutations considerably increased from 0.35 (at diagnosis) to 0.76 (at relapse). This increase was most plausibly caused by a selective pressure of therapy, which resulted in the survival, overgrowth and spread of subclones with *TP53* mutation (a "selective pressure" hypothesis). According to another hypothesis—MCL subclones at different compartments might have different VAFs of *TP53* mutations already at diagnosis. Survival, overgrowth, and spread of MCL cells with high VAF of *TP53* mutations in such an exclusive compartment would result in increased VAF of *TP53* detected at relapse (a "compartment" hypothesis). Targeted sequencing of *TP53* in different compartments in patients with available DNA (P02, P19, and P20) confirmed low VAF of *TP53* mutations in all tested compartments at diagnosis compared to the relapse thereby supporting the selective pressure hypothesis over the compartment hypothesis (Table S3). In addition, in patients P02 and P19 WES identified two newly detected variants at relapse (*NEGR1* and *EZH2*), which were included in the panel of genes used for the targeted sequencing. The targeted sequencing confirmed that both variants were detected in the relapsed samples, but not in two different diagnostic samples of the analyzed patients (Table S3).

Deletions of *CDKN2A/B* were newly predicted by WES in eight patients at relapse. However, it must be emphasized that WES-based CNV predictions cannot detect smaller clones (i.e., <30%).[42] Indeed, at diagnosis the routine FISH analysis revealed more patients with *CDKN2A* inactivation compared to WES-based CNV prediction (15 patients compared to 10 patients). The CNV data thus suggest that smaller MCL subclones with *CDKN2A* deletion were plausibly not predicted by WES at diagnosis (because they were too small) but were successfully predicted after therapy-driven selection and overgrowth of *CDKN2A*-deleted MCL clones at relapse. Our current, as well as previous observations thus confirm a critical role of *CDKN2A/B* deletions in mediating chemoresistant phenotype of MCL cells and suggest *CDKN2A/B* deletions are later (subclonal) events, which plausibly occur within *TP53* mutated MCL clones.[40] Our WES data (both variants and CNVs) thus suggest a selection of pre-existing MCL (sub) clones with inactivated DNA damage response pathways ($TP53_{mut/del}$, $CDKN2A_{del}$) after failure of standard front-line immunochemotherapy, which is consistent with the so far published data.[5,8,10,40]

Besides the observed genetic losses, CNV predictions also identified recurrent amplifications of important oncogenes, for example, *PIK3CA* coding for p110α subunit of a phosphatidylinositol 3-kinase (*PI3K*). *PIK3CA* gains belonged to the most significant CNVs detected both at diagnosis (46% patients) and relapse (50% patients), which confirmed the already published findings.[43,44] The *PIK3CA* gains, together with frequently observed losses of *GNA14*, and forkhead box O3 (*FOXO3*) genes suggest dysregulation of the PI3K-AKT pathway in MCL, both at diagnosis, and (even more) at relapse.[45,46]

The most frequent newly mutated gene at relapse was a tumor suppressor low-density lipoprotein receptor-related protein 1B (*LRP1B*, 3 new variants in 2 patients, in total 6 out of 25 patients at relapse, 28%). Inactivation of *LRP1B* by diverse genetic and epigenetic mechanisms belongs to the most frequent alternations in human cancer overall.[47] Recurrent alterations of *LRP1B* gene were also reported in different lymphoma subtypes, including diffuse large B-cell lymphoma (DLBCL), mucosa associated lymphoid tissue (MALT) lymphoma, transformation of follicular lymphoma to DLBCL, or primary central nervous system lymphomas (PCNSL).[48–52] Mutations of *LRP1B* correlated with a higher total mutational burden in patients with PCNSL, hepatocellular carcinoma, or melanoma.[51,53,54] In primary gastrointestinal DLBCL, mutations of *LRP1B* correlated with significantly worse OS.[48] Of note, *LRP1B* mutations correlated with favorable response to immune checkpoint inhibitors across diverse cancer types including DLBCL.[55,56] Despite that *LRP1B* belongs to established tumor suppressors, its precise role in the biology of MCL (and other lymphomas), and its potential application as a prognostic or predictive factor remain to be elucidated in larger patient cohorts and functional translational studies. Mutations of *KMT2D* found frequently at diagnosis and newly in two patients at relapse (in total 8 out of 25 patients at relapse, 32%) are known to correlate with adverse prognosis in MCL.[10] In addition to *LRP1B* and *KMT2D*, we identified several other candidate genes found newly mutated in at least two out of 25 patients at relapse, including *HOXD9*, *CDC27*, *RYR2*, and *FLNA* genes. Despite their association with diverse types of cancer, their role as drivers of MCL progression remain elusive.[57–61]

In summary, our data brought evidence on drastic clonal evolution of MCL after failure of standard front-line immunochemotherapy. Our data suggest that chemotherapy-resistant (sub)clones enriched in aberrations of prognostically adverse genes were plausibly present already at diagnosis in majority (if not all) cases. Importantly, the selected chemotherapy-resistant lymphoma populations at relapse were not only enriched in inactivation of genes regulating DNA damage response pathways (i.e., *TP53* and *CDKN2A/B*) but also were significantly more genetically heterogeneous compared to the diagnostic samples (i.e., more variants, larger CNVs). Our data clearly confirm insufficient efficacy of chemotherapy in the patients with *TP53* and *CDKN2A* inactivation (i.e., C4 cluster disease), and indicate these patients might profit from earlier administration of innovative treatments including immunotherapy with genetically modified autologous T-cells. Finally, our study confirmed several potential drivers of MCL relapse including *LRP1B*, *KMT2D*, *SP140*, *NOTCH1/2*, *PIK3CA*, or *GNA14*, which provides a sound background for proof-of-concept translational studies.

AUTHOR CONTRIBUTIONS

Jana Karolová designed and performed research, analyzed the data, and wrote the paper. Dmitry Kazantsev performed research and analyzed the data. Michael Svatoň analyzed the data and aided in the design of the research. Liliana Tušková, Kristína Forsterová, Diana Maláriková, Kateřina Benešová, Tomáš Heizer, Alexandra Dolníková, Lucie Winkowska, and Karla Svobodová contributed to the sample processing and analysis. Jan Hojný and Eva Krkavcová contributed to sample processing for targeted sequencing and analysis of data. Magdalena Klanová, Eva Froňková, Zuzana Zemanová, and Marek Trněný provided critical assessment of the study. Pavel Klener designed the research, provided critical assessment of the study, and wrote the paper.

ACKNOWLEDGMENTS

We would like to thank all patients who participated in this project. This study was supported by Czech Health Research Council grant number AZV NU21-03-00386, Grant agency of the Czech Republic grant GA23-05377S, and the project National Institute for Cancer Research (Programme EXCELES, ID Project No. LX22NPO5102)—Funded by the European Union – Next Generation EU. This work was also supported by the Cooperatio Program, research area "Hematooncology" and Charles University graduate students research program (acronym SVV) No. 260634/2023 and partly by the project MH CZ-DRO-VFN64165 (Ministry of Health, Czech Republic).

CONFLICT OF INTEREST STATEMENT

The authors declare no conflicts of interest.

DATA AVAILABILITY STATEMENT

Original data are available upon reasonable request. Please, contact jana.karolova@vfn.cz. A complete list of variants filtered out during the analysis is available in Table S1 under the link: https://doi.org/10.5281/zenodo.7473496.

ORCID

J. Karolová https://orcid.org/0000-0003-3828-6000
P. Klener https://orcid.org/0000-0001-7786-9378

REFERENCES

1. Swerdlow SH, Campo E, Pileri SA, et al. The 2016 revision of the World Health Organization classification of lymphoid neoplasms. *Blood*. 2016;127(20):2375-2390.
2. Jain P, Wang ML. Mantle cell lymphoma in 2022—a comprehensive update on molecular pathogenesis, risk stratification, clinical approach, and current and novel treatments. *Am J Hematol*. 2022;97(5):638-656.
3. Eyre TA, Cheah CY, Wang ML. Therapeutic options for relapsed/refractory mantle cell lymphoma. *Blood*. 2022;139(5):666-677.
4. Zhang J, Jima D, Moffitt AB, et al. The genomic landscape of mantle cell lymphoma is related to the epigenetically determined chromatin state of normal B cells. *Blood*. 2014;123(19):2988-2996.
5. Hill HA, Qi X, Jain P, et al. Genetic mutations and features of mantle cell lymphoma: a systematic review and meta-analysis. *Blood Adv*. 2020;4(13):2927-2938.
6. Bea S, Salaverria I, Armengol L, et al. Uniparental disomies, homozygous deletions, amplifications, and target genes in mantle cell lymphoma revealed by integrative high-resolution whole-genome profiling. *Blood*. 2009;113(13):3059-3069.
7. Beà S, Valdés-Mas R, Navarro A, et al. Landscape of somatic mutations and clonal evolution in mantle cell lymphoma. *Proc Natl Acad Sci U S A*. 2013;110(45):18250-18255.
8. Eskelund CW, Dahl C, Hansen JW, et al. TP53 mutations identify younger mantle cell lymphoma patients who do not benefit from intensive chemoimmunotherapy. *Blood*. 2017;130(17):1903-1910.
9. Nadeu F, Martin-Garcia D, Clot G, et al. Genomic and epigenomic insights into the origin, pathogenesis, and clinical behavior of mantle cell lymphoma subtypes. *Blood*. 2020;136(12):1419-1432.
10. Ferrero S, Rossi D, Rinaldi A, et al. KMT2D mutations and TP53 disruptions are poor prognostic biomarkers in mantle cell lymphoma receiving high-dose therapy: a FIL study. *Haematologica*. 2020;105(6):1604-1612.
11. Pararajalingam P, Coyle KM, Arthur SE, et al. Coding and noncoding drivers of mantle cell lymphoma identified through exome and genome sequencing. *Blood*. 2020;136(5):572-584.
12. Kridel R, Meissner B, Rogic S, et al. Whole transcriptome sequencing reveals recurrent NOTCH1 mutations in mantle cell lymphoma. *Blood*. 2012;119(9):1963-1971.
13. Le Bris Y, Magrangeas F, Moreau A, et al. Whole genome copy number analysis in search of new prognostic biomarkers in first line treatment of mantle cell lymphoma. A study by the LYSA group. *Hematol Oncol*. 2020;38(4):446-455.
14. Halldórsdóttir AM, Sander B, Göransson H, et al. High-resolution genomic screening in mantle cell lymphoma—specific changes correlate with genomic complexity, the proliferation signature and survival. *Genes Chromosomes Cancer*. 2011;50(2):113-121.
15. Streich L, Sukhanova M, Lu X, et al. Aggressive morphologic variants of mantle cell lymphoma characterized with high genomic instability showing frequent chromothripsis, CDKN2A/B loss, and TP53 mutations: a multi-institutional study. *Genes Chromosomes Cancer*. 2020;59(8):484-494.
16. Yi S, Yan Y, Jin M, et al. Genomic and transcriptomic profiling reveals distinct molecular subsets associated with outcomes in mantle cell lymphoma. *J Clin Invest*. 2022;132(3):e153283.
17. Li H, Durbin R. Fast and accurate short read alignment with burrows-wheeler transform. *Bioinformatics*. 2009;25(14):1754-1760.
18. Danecek P, Bonfield JK, Liddle J, et al. Twelve years of SAMtools and BCFtools. *GigaScience*. 2021;10(2):giab008.
19. Koboldt DC, Zhang Q, Larson DE, et al. VarScan 2: somatic mutation and copy number alteration discovery in cancer by exome sequencing. *Genome Res*. 2012;22(3):568-576.
20. Cingolani P, Platts A, Wang LL, et al. A program for annotating and predicting the effects of single nucleotide polymorphisms, SnpEff. *Fly*. 2012;6(2):80-92.
21. Robinson JT, Thorvaldsdóttir H, Winckler W, et al. Integrative genomics viewer. *Nat Biotechnol*. 2011;29(1):24-26.
22. Thorvaldsdóttir H, Robinson JT, Mesirov JP. Integrative genomics viewer (IGV): high-performance genomics data visualization and exploration. *Brief Bioinform*. 2012;14(2):178-192.
23. Gu Z. Complex heatmap visualization. *iMeta*. 2022;1(3):e43.
24. Mayakonda A, Lin DC, Assenov Y, Plass C, Koeffler HP. Maftools: efficient and comprehensive analysis of somatic variants in cancer. *Genome Res*. 2018;28(11):1747-1756.
25. Talevich E, Shain AH, Botton T, Bastian BC. CNVkit: genome-wide copy number detection and visualization from targeted DNA sequencing. *PLoS Comput Biol*. 2016;12(4):e1004873.
26. Tibshirani R, Wang P. Spatial smoothing and hot spot detection for CGH data using the fused lasso. *Biostatistics*. 2008;9(1):18-29.
27. Mermel CH, Schumacher SE, Hill B, Meyerson ML, Beroukhim R, Getz G. GISTIC2.0 facilitates sensitive and confident localization of the targets of focal somatic copy-number alteration in human cancers. *Genome Biol*. 2011;12(4):R41.
28. Yang P, Zhang W, Wang J, Liu Y, An R, Jing H. Genomic landscape and prognostic analysis of mantle cell lymphoma. *Cancer Gene Ther*. 2018;25(5–6):129-140.
29. Royo C, Salaverria I, Hartmann EM, Rosenwald A, Campo E, Beà S. The complex landscape of genetic alterations in mantle cell lymphoma. *Semin Cancer Biol*. 2011;21(5):322-334.
30. Wu C, de Miranda NF, Chen L, et al. Genetic heterogeneity in primary and relapsed mantle cell lymphomas: impact of recurrent CARD11 mutations. *Oncotarget*. 2016;7(25):38180-38190.
31. Ahmed M, Zhang L, Nomie K, Lam L, Wang M. Gene mutations and actionable genetic lesions in mantle cell lymphoma. *Oncotarget*. 2016;7(36):58638-58648.
32. Zhang Q, Wang HY, Liu X, et al. Dynamic changes in gene mutational landscape with preservation of core mutations in mantle cell lymphoma cells. *Front Oncol*. 2019;9:568.

33. Geisler CH, Kolstad A, Laurell A, et al. Long-term progression-free survival of mantle cell lymphoma after intensive front-line immunochemotherapy with in vivo-purged stem cell rescue: a nonrandomized phase 2 multicenter study by the Nordic Lymphoma Group. *Blood*. 2008;112(7):2687-2693.
34. Geisler CH, Kolstad A, Laurell A, et al. Nordic MCL2 trial update: six-year follow-up after intensive immunochemotherapy for untreated mantle cell lymphoma followed by BEAM or BEAC + autologous stem-cell support: still very long survival but late relapses do occur. *Br J Haematol*. 2012;158(3):355-362.
35. Salaverria I, Zettl A, Bea S, et al. Specific secondary genetic alterations in mantle cell lymphoma provide prognostic information independent of the gene expression-based proliferation signature. *J Clin Oncol*. 2007;25(10):1216-1222.
36. Bea S, Ribas M, Hernandez JM, et al. Increased number of chromosomal imbalances and high-level DNA amplifications in mantle cell lymphoma are associated with blastoid variants. *Blood*. 1999;93(12):4365-4374.
37. Jakša R, Karolová J, Svatoň M, et al. Complex genetic and histopathological study of 15 patient-derived xenografts of aggressive lymphomas. *Lab Invest*. 2022;102:957-965.
38. Greiner TC, Dasgupta C, Ho VV, et al. Mutation and genomic deletion status of ataxia telangiectasia mutated (ATM) and p53 confer specific gene expression profiles in mantle cell lymphoma. *Proc Natl Acad Sci U S A*. 2006;103(7):2352-2357.
39. Mareckova A, Malcikova J, Tom N, et al. ATM and TP53 mutations show mutual exclusivity but distinct clinical impact in mantle cell lymphoma patients. *Leuk Lymphoma*. 2019;60(6):1420-1428.
40. Malarikova D, Berkova A, Obr A, et al. Concurrent TP53 and CDKN2A gene aberrations in newly diagnosed mantle cell lymphoma correlate with chemoresistance and call for innovative upfront therapy. *Cancers (Basel)*. 2020;12(8):2120.
41. Silkenstedt E, Arenas F, Colom-Sanmartí B, et al. Notch1 signaling in NOTCH1-mutated mantle cell lymphoma depends on Delta-Like ligand 4 and is a potential target for specific antibody therapy. *J Exp Clin Cancer Res*. 2019;38(1):446.
42. Sandmann S, Wöste M, de Graaf AO, Burkhardt B, Jansen JH, Dugas M. CopyDetective: detection threshold-aware copy number variant calling in whole-exome sequencing data. *Gigascience*. 2020;9(11):giaa118.
43. Psyrri A, Papageorgiou S, Liakata E, et al. Phosphatidylinositol 3′-kinase catalytic subunit alpha gene amplification contributes to the pathogenesis of mantle cell lymphoma. *Clin Cancer Res*. 2009;15(18):5724-5732.
44. Iyengar S, Clear A, Bödör C, et al. P110α-mediated constitutive PI3K signaling limits the efficacy of p110δ-selective inhibition in mantle cell lymphoma, particularly with multiple relapse. *Blood*. 2013;121(12):2274-2284.
45. Obrador-Hevia A, Serra-Sitjar M, Rodríguez J, Villalonga P, Fernández de Mattos S. The tumour suppressor FOXO3 is a key regulator of mantle cell lymphoma proliferation and survival. *Br J Haematol*. 2012;156(3):334-345.
46. Xu C, Li YM, Sun B, Zhong FJ, Yang LY. GNA14's interaction with RACK1 inhibits hepatocellular carcinoma progression through reducing MAPK/JNK and PI3K/AKT signaling pathway. *Carcinogenesis*. 2021;42(11):1357-1369.
47. Príncipe C, Dionísio de Sousa IJ, Prazeres H, Soares P, Lima RT. LRP1B: a giant lost in cancer translation. *Pharmaceuticals (Basel)*. 2021;14(9):836.
48. Li SS, Zhai XH, Liu HL, et al. Whole-exome sequencing analysis identifies distinct mutational profile and novel prognostic biomarkers in primary gastrointestinal diffuse large B-cell lymphoma. *Exp Hematol Oncol*. 2022;11(1):71.
49. Cascione L, Rinaldi A, Bruscaggin A, et al. Novel insights into the genetics and epigenetics of MALT lymphoma unveiled by next generation sequencing analyses. *Haematologica*. 2019;104(12):e558-e561.
50. González-Rincón J, Méndez M, Gómez S, et al. Unraveling transformation of follicular lymphoma to diffuse large B-cell lymphoma. *PloS One*. 2019;14(2):e0212813.
51. Zhang R, Wei B, Hu Y, et al. Whole-exome sequencing revealed the mutational profiles of primary central nervous system lymphoma. *Clin Lymphoma Myeloma Leuk*. 2023;23(4):291-302.
52. Schaffer M, Chaturvedi S, Davis C, et al. Activity of ibrutinib plus R-CHOP in diffuse large B-cell lymphoma: response, pharmacodynamic, and biomarker analyses of a phase Ib study. *Cancer Treat Res Commun*. 2020;25:100235.
53. Liu F, Hou W, Liang J, Zhu L, Luo C. LRP1B mutation: a novel independent prognostic factor and a predictive tumor mutation burden in hepatocellular carcinoma. *J Cancer*. 2021;12(13):4039-4048.
54. Chen H, Chong W, Wu Q, Yao Y, Mao M, Wang X. Association of LRP1B mutation with tumor mutation burden and outcomes in melanoma and non-small cell lung cancer patients treated with immune check-point blockades. *Front Immunol*. 2019;10:1113.
55. Brown LC, Tucker MD, Sedhom R, et al. LRP1B mutations are associated with favorable outcomes to immune checkpoint inhibitors across multiple cancer types. *J Immunother Cancer*. 2021;9(3):e001792.
56. Hodkinson BP, Schaffer M, Brody JD, et al. Biomarkers of response to ibrutinib plus nivolumab in relapsed diffuse large B-cell lymphoma, follicular lymphoma, or Richter's transformation. *Transl Oncol*. 2021;14(1):100977.
57. Zhu H, Dai W, Li J, et al. HOXD9 promotes the growth, invasion and metastasis of gastric cancer cells by transcriptional activation of RUFY3. *J Exp Clin Cancer Res*. 2019;38(1):412.
58. Song Y, Song W, Li Z, et al. CDC27 promotes tumor progression and affects PD-L1 expression in T-cell lymphoblastic lymphoma. *Front Oncol*. 2020;10:488.
59. Xu N, Zhang D, Chen J, He G, Gao L. Low expression of ryanodine receptor 2 is associated with poor prognosis in thyroid carcinoma. *Oncol Lett*. 2019;18(4):3605-3612.
60. Wang A, Liu L, Yuan M, et al. Role and mechanism of FLNa and UCP2 in the development of cervical cancer. *Oncol Rep*. 2020;44(6):2656-2668.
61. Nagasaka M, Inoue Y, Yoshida M, et al. The deubiquitinating enzyme USP17 regulates c-Myc levels and controls cell proliferation and glycolysis. *FEBS Lett*. 2022;596(4):465-478.
62. Klener P, Fronkova E, Belada D, et al. Alternating R-CHOP and R-cytarabine is a safe and effective regimen for transplant-ineligible patients with a newly diagnosed mantle cell lymphoma. *Hematol Oncol*. 2018;36(1):110-115.

SUPPORTING INFORMATION

Additional supporting information can be found online in the Supporting Information section at the end of this article.

How to cite this article: Karolová J, Kazantsev D, Svatoň M, et al. Sequencing-based analysis of clonal evolution of 25 mantle cell lymphoma patients at diagnosis and after failure of standard immunochemotherapy. *Am J Hematol*. 2023;98(10):1627-1636. doi:10.1002/ajh.27044